Comparison of Multidirectional Representations for Multispectral Palmprint Recognition

Zohaib Khan(✉), Faisal Shafait, and Ajmal Mian

School of Computer Science and Software Engineering,
The University of Western Australia, Perth, Australia
{zohaib.khan,faisal.shafait,ajmal.mian}@uwa.edu.au

Abstract. Palmprint is emerging as a new multi-modal biometric for human recognition. Multispectral palmprint images captured in the visible and infrared spectrum not only contain the superficial structure of a palm, but also the underlying structure of veins; making them a highly discriminating person identifier. This study comparatively analyzes multidirectional representations for multispectral palmprint recognition which show promising results. Comprehensive experiments for both identification and verification scenarios are performed on three public datasets. The accuracies of state-of-the-art clearly indicate the viability of multidirectional coding methods for multispectral palmprint recognition.

1 Introduction

The information present in a human palm has an immense amount of potential for biometric recognition. Information visible to the naked eye includes the principal lines, the wrinkles and the fine ridges which form a unique pattern for every individual [13]. These superficial features can be captured using standard imaging devices. High resolution scanners capture the fine ridge pattern of a palm which is generally employed for latent palmprint identification in forensics [3]. The principal lines and wrinkles acquired with low resolution sensors are suitable for security applications like user identification or authentication [12].

Additional information present in the human palm is the subsurface vein pattern which is indifferent to the palm lines. Such features cannot be easily acquired by a standard imaging sensor. Infrared imaging can capture subsurface features due to its capability to penetrate the human skin. The superficial and subsurface features of a palm have been collectively investigated under the subject of *'multispectral palmprint recognition'*. Using *Multispectral Imaging (MSI)*, it is possible to capture images of an object at multiple wavelengths of light, in the visible spectrum and beyond. A monochromatic camera under spectrally varying illuminations can acquire multispectral palm images. Figure 1 shows palm images captured at three different wavelengths. The availability of such complementary features (palm lines and veins) makes palmprint suitable for recognition where user cooperation is affordable, e.g., at secure access gates, workplace attendance and identification records.

U. Garain and F. Shafait (Eds.): IWCF 2012 and 2014, LNCS 8915, pp. 44–54, 2015.
DOI: 10.1007/978-3-319-20125-2_5

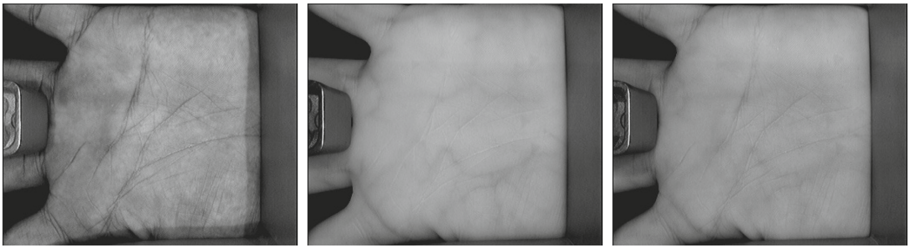

(a) *Lines* (470nm) (b) *Veins* (880nm) (c) *Both* (660nm)

Fig. 1. Examples of palmprint features in multiple bands. Three bands of a multispectral image captured using a contact based sensor. (a) Palm lines captured in the visible range. (b) Palm veins captured in the near infrared range. (c) A combination of the line and vein features at intermediate wavelengths.

The multi-modal nature of multispectral palmprints requires robust feature extraction methods. This work compares state-of-the-art orientation codes for *multispectral palmprint recognition*. Section 2 briefly describes the concept of orientation coding algorithms with details of the Contour Code (ContCode) [4], the Competitive Code (CompCode) [6], the Ordinal Code (OrdCode) [8] and the Derivative of Gaussian Code (DoGCode) [9]. Section 4 presents the multispectral palmprint verification and identification in various experimental settings and compares the performance of the state-of-the-art. These experiments are performed on three publicly available multispectral palmprint databases i.e. PolyU-Multispectral Palmprint Database, PolyU-Hyperspectral Palmprint Database and CASIA Multispectral Palmprint Database described in Sect. 3. Section 6 ends the paper with conclusions.

2 Multidirectional Palmprint Encoding

Palmprint recognition approaches can be categorized into line-like feature detectors, subspace learning methods and texture based coding techniques [5]. These three categories are not mutually exclusive and their combinations are also possible. Line detection based approaches commonly extract palm lines using edge detectors [2]. Recognition based solely on palm lines proves insufficient due to their sparse nature and the possibility of different individuals having highly similar palm lines [11]. Although, line detection can extract palm lines effectively, it may not be equally useful for the extraction of palm veins due to their low contrast and broad structure. A subspace projection captures the local and/or global characteristics of a palm by projecting to the most varying [7] or the most discriminative [10] dimensions. The palmprint subspace representations are not effective compared to the state-of-the-art techniques. The main reason is that subspaces learned from misaligned palms are unlikely to generate accurate representation of each identity.

2.1 Orientation Coding

Orientation codes extract and encode the orientation of lines which have shown state-of-the-art performance in palmprint recognition [13]. In the generic form of orientation coding, the response of a palm to a bank of directional filters is computed such that the resulting directional subbands correspond to specific orientations of line. Then, the dominant orientation index from the directional subbands is extracted at each point to form the orientation code. Orientation codes can be binarized for efficient storage and fast matching unlike other representations which require floating point data storage and computations.

Derivative of Gaussian Code (DoGCode) [9] is a compact representation which only uses vertical and horizontal gaussian derivative filters to extract feature orientation of a palmprint image, and then encodes the filter responses into binary code. The horizontal and vertical derivatives of 2D Gaussian filters used in DoGCode are given as

$$\mathcal{F}_x(x, y : \sigma) = -\frac{x}{2\pi\sigma^4} e^{\left(-\frac{x^2+y^2}{2\sigma^2}\right)} \tag{1}$$

$$\mathcal{F}_y(x, y : \sigma) = -\frac{y}{2\pi\sigma^4} e^{\left(-\frac{x^2+y^2}{2\sigma^2}\right)} \tag{2}$$

where σ is the scale of the filter.

Ordinal Code (OrdCode) [8] emphasizes the ordinal relationship of lines by comparing mutually orthogonal filter pairs to extract the feature orientation at a point. It uses six 2D elliptical Gaussian filters for filtering the palmprint image. The 2D elliptical Gaussian filter used in the OrdCode are defined as

$$\mathcal{F}(x, y : \theta, \delta_x, \delta_y) = e^{-\left(\frac{x\cos\theta + y\sin\theta}{\delta_x}\right)^2 - \left(\frac{-x\sin\theta + y\cos\theta}{\delta_y}\right)^2} \tag{3}$$

where (δ_x, δ_y) are the scales of the orthogonal Gaussian filters oriented at $(\theta, \theta + \pi/2)$. The ratio δ_x/δ_y is kept high to get an elliptical filter response.

Competitive Code (CompCode) [6] employs a directional bank of Gabor filters to extract the orientation of palm lines. The 2D Gabor filters for multidirectional filtering of palm images are given as

$$\mathcal{F}(x, y : \theta, \omega, \kappa) = -\frac{\omega}{\sqrt{2\pi}\kappa} e^{\frac{\omega^2}{8\kappa^2}(4(x\cos\theta + y\sin\theta)^2 + (-x\sin\theta + y\cos\theta)^2)} \left(e^{\iota\omega x} - e^{-\frac{\kappa^2}{2}}\right) \tag{4}$$

where $\omega = \kappa/\sigma$ is the radial frequency and θ is the orientation of the Gabor filter. The parameter $\kappa = \sqrt{2\log 2}\frac{2\delta+1}{2\delta-1}$, where δ is the bandwidth of the filter response.

Contour Code (ContCode) [4] uses pyramidal-directional filter banks to extract the orientation of palmprint features and uses a binary hash table encoding for efficient storage and matching. The pyramidal bandpass filter captures the details in the palm at a single scale. The pyramidal filtered component is subsequently convolved with a 2D directional filter bank of sinc filter.

$$\mathcal{F}(x,y:\theta) = P_f(x,y) * \frac{1}{\sqrt{2}} \frac{sin(x:\theta)}{x} \frac{sin(y:\theta)}{y} \ , \tag{5}$$

where $P_f(x,y)$ is the pyramidal filter. The combination of pyramidal and directional filter decomposition stages robustly capture line like features from palmprints.

2.2 Binary Encoding and Matching

Orientation codes can be integer coded according to the maximum (or minimum) filter response for directional subband at orientation θ

$$C(x,y) = \arg\min_{i} \quad I(x,y) * \mathcal{F}(x,y:\theta) \ , \tag{6}$$

where $\theta = i\frac{\pi}{K}$ where K is the total number of orientations. For storage and matching, orientation codes can be binarized and stored in efficient structures such as one proposed in [4]. All methods in this paper use the same binary encoding and matching scheme for a fair comparison.

3 Multispectral Palmprint Databases

Experiments are performed on the PolyU-MS[1], PolyU-HS[2] and CASIA-MS[3] palmprint databases. All databases contain low resolution (<150 *dpi*) palmprint images. Several samples of each subject were acquired in two different sessions. Detailed specifications of the databases are given in Table 1.

The PolyU-HS database was collected with the aim to find the minimum number of bands required for designing a multispectral palmprint recognition system rather than utilizing the complete set of hyperspectral bands. The number of bands of the PolyU-HS database were reduced from 69 to 4 according to the band selection method proposed in [1]. The four most informative bands were 580 nm, 620 nm, 760 nm and 940 nm.

[1] PolyU Multispectral Palmprint Database http://www.comp.polyu.edu.hk/~biometrics/MultispectralPalmprint/MSP.htm.
[2] PolyU Hyperspectral Palmprint Database http://www4.comp.polyu.edu.hk/~biometrics/HyperspectralPalmprint/HSP.htm.
[3] CASIA Multispectral Palmprint Database http://www.cbsr.ia.ac.cn/MS_Palmprint_Database.asp.

Table 1. Specifications of the PolyU-MS, PolyU-HS and CASIA-MS databases.

Database	PolyU-MS	PolyU-HS	CASIA-MS
Sensor type	contact	contact	non-contact
Identities	500	380	200
Samples per identity	12	11–14	6
Total samples	6000	5240	1200
Bands per sample	4	69	6
Wavelength(nm)	470, 525, 660, 880	420–1100 (10 nm steps)	460, 630, 700, 850, 940, White

Table 2. Individual performance of bands in PolyU-MS, PolyU-HS and CASIA-MS database.

PolyU-MS

Band	GAR(%)	EER(%)
470 nm	99.94	0.0784
525 nm	99.98	0.0420
660 nm	99.99	0.0242
880 nm	99.90	0.1030

PolyU-HS

Band	GAR(%)	EER(%)
580 nm	99.56	0.3003
620 nm	99.93	0.0779
760 nm	99.67	0.2475
940 nm	99.83	0.1495

CASIA-MS

Band	GAR(%)	EER(%)
460 nm	88.95	2.9246
630 nm	87.79	3.9065
700 nm	57.35	9.7318
850 nm	87.45	4.1398
940 nm	90.73	3.4769

4 Multispectral Palmprint Recognition

The multispectral palm regions in each band are downsampled to 32×32 pixels using bi-cubic interpolation. Then, features are extracted using four state-of-the-art methods for subsequent use in recognition experiments.

4.1 Verification Experiments

Verification experiments are performed on PolyU-MS, PolyU-HS and CASIA-MS databases adapting the protocol of [13], where session based experiments are structured to observe the recognition performance. The evaluation comprises five verification experiments to test different techniques. The experiments proceed by matching

Exp.1: individual bands of palm irrespective of the session.
Exp.2: multispectral palmprints acquired in the 1st session.
Exp.3: multispectral palmprints acquired in the 2nd session.
Exp.4: multispectral palmprints of the 1st session to the 2nd session.
Exp.5: multispectral palmprints irrespective of the session (all vs. all).

In all experiments, the ROC curves, which depict the False Rejection Rate (FRR) versus the False Acceptance Rate (FAR) are reported. The Equal Error Rate (EER), and the Genuine Acceptance Rate (GAR) at 0.1 % FAR are also summarized to compare performance of the state-of-the-art techniques.

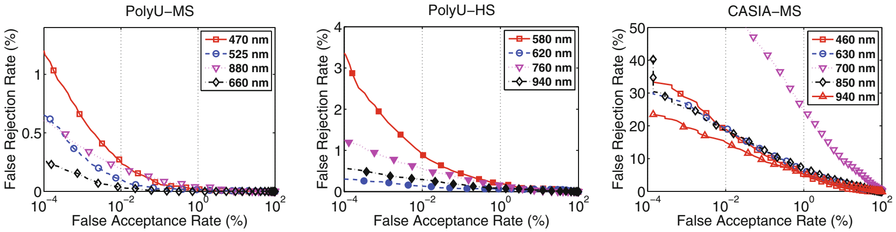

Fig. 2. Exp.1: ROC curves of ContCode on individual bands

Experiment 1: Band Discriminant Capability. This experiment compares the relative discriminant capability of individual bands in different databases. We compare the performance of individual bands of the PolyU-MS and CASIA-MS database using ContCode. Figure 2 shows the ROC curves of the individual bands and Table 2 lists their EERs. In the PolyU-MS database, the 660 nm band gives the best performance indicating the presence of more discriminatory features. A logical explanation could be that the 660 nm wavelength partially captures both the line and vein features making this band relatively more discriminative. In the PolyU-HS database, the 620 nm and 940 nm have the lowest errors followed by 760 nm and 580 nm. In CASIA-MS database, the most discriminant information is present in the 940 nm, 850 nm, 630 nm and 460 nm bands which are close competitors.

Experiment 2: Verification in the 1st Session This experiment analyzes the variability in the palmprint data acquired in the 1st session. Figure 3 compares the ROC curves of the ContCode with three other techniques on all databases. It is observable that the CompCode and the OrdCode show intermediate performance close to ContCode. The DoGCode exhibits a drastic degradation of accuracy implying its inability to sufficiently cope with the variations of CASIA-MS data. Overall, the CompCode and ContCode perform better on both databases while the latter performs the best.

Experiment 3: Verification in the 2nd Session This experiment analyzes the variability in the palmprint data acquired in the 2nd session. This allows for a comparison with the results of *Exp.2* to analyze the intra-session variability.

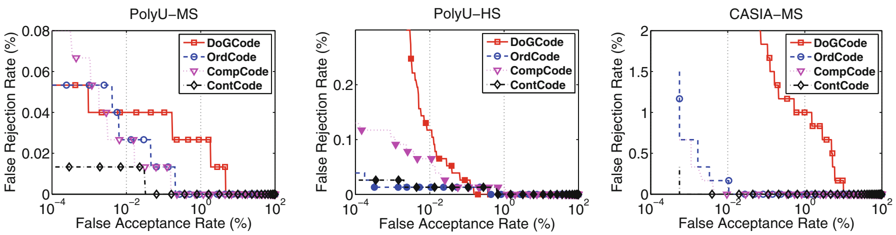

Fig. 3. Exp.2: Matching palmprints of 1st session.

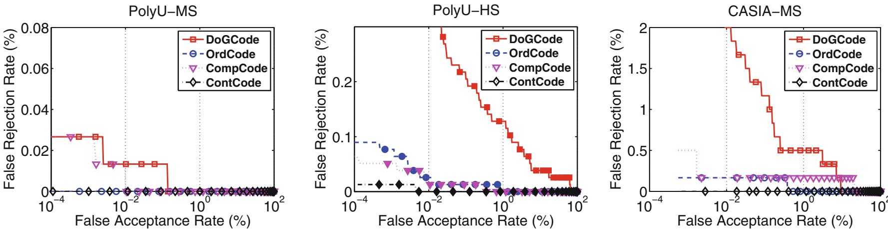

Fig. 4. Exp.3: Matching palmprints of 2^{nd} session.

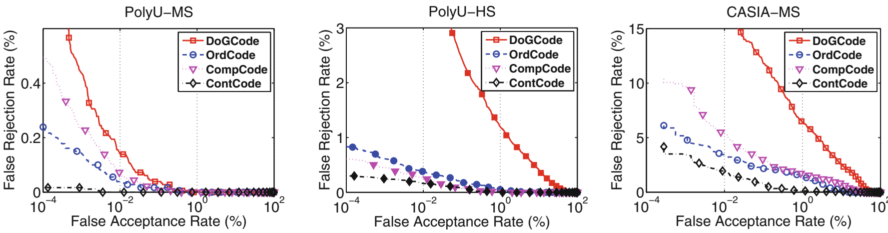

Fig. 5. Exp.4: Matching palmprints of the 1^{st} session to the 2^{nd} session. The verification performance is low relative to *Exp.2* and *Exp.3*. However, the performance degradation of the proposed ContCode is much less than the other techniques on both databases, indicating its robustness to image variability.

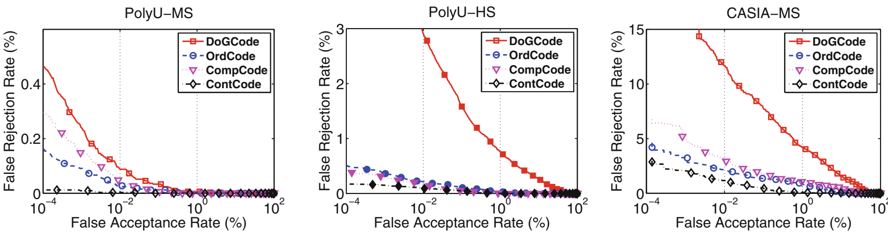

Fig. 6. Exp.5: Matching palmprints irrespective of the acquisition session.

Therefore, only the palmprints acquired in the 2^{nd} session are matched. Figure 4 compares the ROC curves of all techniques. The small improvement in verification performance on the images of 2^{nd} session can be attributed to the better quality of images and increased user familiarity with the acquisition system.

Experiment 4: Verification of 2^{nd} Session from 1^{st} Session This experiment mimics a verification scenario which incurs variation in image quality due to sensor aging or subject behavior over time. It analyzes the inter-session variability of multispectral palmprints. Therefore, all images from the 1^{st} session are matched to all images of the 2^{nd} session. Figure 5 compares the ROC curves of the techniques on all databases. Note that the performance of all techniques is relatively lower for this experiment compared to *Exp.2* and *Exp.3* because this

Table 3. Summary of verification results for *Exp.2* to *Exp.5*

		PolyU-MS			
		DoGCode	OrdCode	CompCode	ContCode
Exp.2	EER(%)	0.0400	0.0267	0.0165	0.0133
	GAR(%)	99.96	99.99	99.99	100.00
Exp.3	EER(%)	0.0133	0	0.0098	0
	GAR(%)	99.99	100.00	100.00	100.00
Exp.4	EER(%)	0.0528	0.0247	0.0333	0.0029
	GAR(%)	99.96	99.98	99.99	100.00
Exp.5	EER(%)	0.0455	0.0212	0.0263	0.0030
	GAR(%)	99.97	99.99	99.99	100.00
		PolyU-HS			
		DoGCode	OrdCode	CompCode	ContCode
Exp.2	EER(%)	0.0398	0.0130	0.0261	0.0130
	GAR(%)	99.97	99.99	99.99	99.99
Exp.3	EER(%)	0.1912	0.0128	0.0128	0.0045
	GAR(%)	99.79	99.99	99.99	100.00
Exp.4	EER(%)	1.1530	0.1598	0.0830	0.0866
	GAR(%)	97.56	99.80	99.93	99.92
Exp.5	EER(%)	0.8150	0.1043	0.0626	0.0596
	GAR(%)	98.42	99.88	99.96	99.96
		CASIA-MS			
		DoGCode	OrdCode	CompCode	ContCode
Exp.2	EER(%)	1.000	0.1667	0.0140	0
	GAR(%)	98.00	99.67	100.00	100.00
Exp.3	EER(%)	0.6667	0.1667	0.1667	0.0011
	GAR(%)	98.50	99.83	99.83	100.00
Exp.4	EER(%)	3.8669	1.2778	0.6667	0.2778
	GAR(%)	87.70	97.39	97.72	99.61
Exp.5	EER(%)	2.8873	0.8667	0.4993	0.2000
	GAR(%)	92.01	98.37	98.60	99.76

is a difficult scenario due to the intrinsic variability in the human behavior over time. However, the drop in performance of ContCode is the minimum. Therefore, it is fair to deduce that ContCode is relatively robust to the image variability over time.

Experiment 5: All-vs-All Verification. This experiment evaluates the overall verification performance by combining images from both sessions. All images

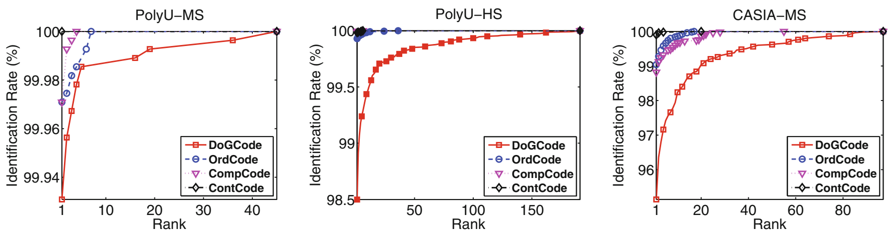

Fig. 7. CMC curves for the identification experiment. Note that ContCode has an average rank-1 recognition rate of 100 % on the PolyU-MS database.

Table 4. Comparison of rank-1 recognition rate and standard deviation on all databases.

Method	PolyU-MS (%)	PolyU-HS (%)	CASIA-MS (%)
DoGCode [9]	99.97±0.04	99.93±0.05	95.08±0.75
OrdCode [8]	99.93±0.05	98.50±0.28	99.02±0.11
CompCode [6]	99.97±0.03	99.99±0.01	99.52±0.11
ContCode [4]	100.0±0	99.98±0.03	99.88±0.08

in the database are matched to all other images, irrespective of the acquisition session which is commonly termed as an "all-versus-all" experiment. Figure 6 compares the ROC curves of all techniques. Similar to the previous experiments, the ContCode consistently outperforms all other techniques.

The results of *Exp.2* to *Exp.5* are summarized in Table 3 for the all databases. The ContCode consistently outperforms the other methods in all experiments. Moreover, CompCode is consistently the second best performer except for very low FAR values in *Exp.4* and *Exp.5* on the PolyU-MS database (see Fig. 5 and Fig. 6). It is also interesting to note that the OrdCode performs better than the DoGCode on all databases.

5 Identification Experiments

Palmprint identification is carried out in 5-fold cross validation experiment and the Cumulative Match Characteristics (CMC) curves are reported alongside the Rank-1 identification rates. The identification rates are averaged over the five folds. In each fold, one multispectral palmprint image per subject is randomly selected to form the gallery and the remaining images are considered as probes. This means that the identification is based on a single multispectral image for each subject in the gallery. This protocol is followed for all databases.

5.1 Experiment 1: Identification Experiment

The CMC curves on all databases are given in Fig. 7 and the identification results are summarized in Table 4. The ContCode achieved an average identification rate of 99.88 % on the CASIA-MS database, 99.91 % on the PolyU-HS database and 100 % on the PolyU-MS database. The ContCode clearly demonstrates better identification performance in comparison to state-of-the-art techniques.

6 Conclusion

In this study, state-of-the-art orientation based coding algorithms were compared for multispectral palmprint recognition. Various experiments were designed to cater for sessional affects in multispectral palmprint recognition. The results indicate that the ContCode is most accurate, followed by CompCode, OrdCode and DoGCode in both verification and identification experiments. Overall, the orientation coding techniques show promising results for extracting multimodal features of a palmprint. The MATLAB code of all techniques including the experiments conducted in this work is available at www.sites.google.com/site/zohaibnet/Home/codes.

Acknowledgements. This research was supported by ARC Grant DP0881813 and DP110102399. Authors acknowledge the Polytechnic University of Hong Kong for providing the PolyU-MS and PolyU-HS Palmprint database and the Chinese Academy of Sciences' Institute of Automation for providing the CASIA MS-PalmprintV1 database.

References

1. Guo, Z., Zhang, D., Zhang, L., Liu, W.: Feature band selection for online multispectral palmprint recognition. IEEE Trans. Inf. Forensics Secur. **7**(3), 1094–1099 (2012)
2. Huang, D.S., Jia, W., Zhang, D.: Palmprint verification based on principal lines. Pattern Recogn. **41**(4), 1316–1328 (2008)
3. Jain, A.K., Feng, J.: Latent palmprint matching. IEEE Trans. Pattern Anal. Mach. Intell. **31**(6), 1032–1047 (2009)
4. Khan, Z., Mian, A., Hu, Y.: Contour code: Robust and efficient multispectral palmprint encoding for human recognition. In: Proceedings of the International Conference on Computer Vision (ICCV), pp. 1935–1942. IEEE (2011)
5. Kong, A., Zhang, D., Kamel, M.: A survey of palmprint recognition. Pattern Recogn. **42**(7), 1408–1418 (2009)
6. Kong, A.K., Zhang, D.: Competitive coding scheme for palmprint verification. In: Proceedings of the International Conference on Pattern Recognition, pp. 520–523. IEEE (2004)
7. Lu, G., Zhang, D., Wang, K.: Palmprint recognition using eigenpalms features. Pattern Recogn. Lett. **24**(9), 1463–1467 (2003)
8. Sun, Z., Tan, T., Wang, Y., Li, S.Z.: Ordinal palmprint representation for personal identification. In: Proceedings of the Computer Vision and Pattern Recognition, pp. 279–284. IEEE (2005)
9. Wu, X., Wang, K., Zhang, D.: Palmprint texture analysis using derivative of gaussian filters. In: Proceedings of the International Conference on Computational Intelligence and Security, pp. 751–754. IEEE (2006)

10. Wu, X., Zhang, D., Wang, K.: Fisherpalms based palmprint recognition. Pattern Recogn. Lett. **24**(15), 2829–2838 (2003)
11. Zhang, D., Guo, Z., Lu, G., Zhang, L., Liu, Y., Zuo, W.: Online joint palmprint and palmvein verification. Expert Syst. Appl. **38**(3), 2621–2631 (2011)
12. Zhang, D., Kong, W.K., You, J., Wong, M.: Online palmprint identification. IEEE Trans. Pattern Anal. Mach. Intell. **25**(9), 1041–1050 (2003)
13. Zhang, D., Zuo, W., Yue, F.: A comparative study of palmprint recognition algorithms. ACM Comput. Surv. (CSUR) **44**(1), 2:1–2:37 (2012)